Dynamic modeling and vibration control for isolation systems based on magnetorheological elastomers

Guanghong Zhu[1*], Zigang Li[1], Hulun Guo[2], Xianxu Bai[3*], Yeping Xiong[4], Ming Li[1]

[1]Department of Mechanics, Xi'an University of Science and Technology, Xi'an 710054, P. R. China

[2]Tianjin Key Laboratory of Nonlinear Dynamics and Control, Department of Mechanics, Tianjin University, Tianjin 300354, P. R. China

[3]Laboratory for Adaptive Structures and Intelligent Systems (LASIS), Department of Vehicle Engineering, Hefei University of Technology, Hefei 230009, China

[4]Faculty of Engineering and the Physical Sciences, University of Southampton, Southampton SO16 7QF, UK

*Corresponding authors.

E-mail addresses: zhuguanghong@xust.edu.cn (G. Zhu), bai@hfut.edu.cn (X. Bai).

Abstract

A fractional rheological model was developed for MRE-based isolation systems to investigate the influence of material elasticity and viscosity on the isolation effect. The identification of model parameters was realized by fitting experimental data of dynamic mechanical analysis for MRE structures. The superior rationality of modeling was reflected with the good consistency and repeatability. The transmissibility was calculated both theoretically and numerically. The method of numerical simulation was verified with an excellent agreement between theoretical and numerical results. The influence of model parameters on transmissibility and energy flow was analyzed to interpret the dynamic behavior of vibration isolation systems. A control strategy based on the coincidence frequency was developed for this MRE-based isolation system to protect the foundation or the sensitive equipment against periodic vibrations. The isolation effect was investigated from the prospect of transmissibility and energy flow. Eventually, the fuzzy control algorithm was adopted to isolate the sensitive equipment against random motions of the ground, and the effectiveness was further validated by comparing with the passive isolation.

Keywords: vibration control, mathematical modeling, magnetorheological elastomers, dynamic mechanical analysis

1 Introduction

The structure on board is liable to respond to excitations from propellers, engines, ancillary machineries and the environment. Excessive vibration may result in the fatigue failure of structures or malfunction of equipment. As for passengers and the crew, the demand of acceptance and habitability is increasing as time goes on. Because

noise and vibration are two main factors in affecting the perception of comfort, vibration control is an important issue for engineering industry. Vibration isolators, a commonly used way to mitigate vibration, conventionally consist of rubber for elastic bearing and energy dissipation (Ibrahim, 2008). Vibration isolation is to protect the foundation against vibration sources, such as rotating machines, or to isolate the sensitive equipment from ground motions. Generally, the dynamic characteristics of installed isolators cannot be changed to adapt to various loading conditions, and the limitation of adaptability makes them fail to satisfy advanced requirements (Yan *et al.*, 2018; Liu *et al.*, 2015).

Various smart materials, such as controllable elastomers, have been used for vibration mitigation as smart elements with different control schemes based on their adjustable dynamic properties. Therefore they have potential for improving the performance of vibration control. Increasing effort has been devoted to making use of smart materials in vibration absorbers and isolators. MRE is composed of magnetizable particles embedded in a non-magnetic rubber matrix, and the mechanical properties of MRE can be controlled rapidly, continuously and reversibly by adjusting magnetic field (Zhu *et al.*, 2019; Sapouna *et al.*, 2017; Kaleta *et al.*, 2011). As a credible alternative to traditional rubber, the advantages of enhanced effectiveness, low cost and good reliability can be obtained by the stiffness variability of MRE-based vibration isolators (Zhu *et al.*, 2021b; Eem *et al.*, 2019; Li and Li, 2019).

A constitutive model, which can accurately present the dynamic performance of MRE, is necessary for the application in vibration control. Initially, the dipole model and the chain model were used to represent the mechanical characteristics of MRE (Davis, 1999; Jolly *et al.*, 1996), and three-dimensional models were subsequently developed (Chen *et al.*, 2007). Those models, which are basically quasi-static, are not sufficient to predict the dynamic behavior of MRE (Wang and Kari, 2019a, 2019b). Experimental results show that the dynamic modulus is dependent on frequency, strain amplitude and temperature (Wan *et al.*, 2019), and those dependencies are often referred to as common phenomena for particle-enhanced rubber. Considering the rheological and viscoelastic properties of MRE, Bouc-Wen model (Bai *et al.*, 2019; Yang *et al.*, 2013) and Ramberg-Osgood model (Zhu *et al.*, 2021b) were developed to represent the hysteretic properties, and the fractional derivative was introduced to describe the dynamic behavior (Poojary and Gangadharan, 2022; Nguyen *et al.*, 2020; Nadzharyan *et al.*, 2018; Graczykowski and PawlOwski, 2017).

Besides the increasing research on modeling of MRE, it has been applied broadly for intelligent devices in varies fields, such as vibration absorbers (Yuan *et al.*, 2019; Kumbhar *et al.*, 2018; Bian *et al.*, 2018; Xin *et al.*, 2017; Qian *et al.*, 2017) and vibration isolators (Fu *et al.*, 2019; Nguyen *et al.*, 2018b; Yu *et al.*, 2015; Yang *et al.*, 2014; Behrooz *et al.*, 2014) due to the frequency shifting property. Several control methods, such as on–off control (Yang *et al.*, 2014), fuzzy control (Fu *et al.*, 2018; Nguyen *et al.*, 2018a), Lyapunov-based seismic control (Behrooz *et al.*, 2014), H-infinity control (Yu *et al.*, 2015) and sliding mode control (Nguyen *et al.*, 2018b) have been employed in control systems based on MRE. Considering that the time delay in control systems may result in unsatisfied effect or system instability, the response time of MRE material was investigated (Zhu *et al.*, 2018). Further more, time compensation strategy and phase compensation strategy were studied for control systems based on MRE (Fu *et al.*, 2020; Yu *et al.*, 2019). There are strategies about delay control for accurate modeling (Wu *et al.*, 2010), but it is difficult to establish accurate models for MRE-based isolation systems with nonlinearity.

As a continuation of a paper (Zhu *et al.*, 2021a), this piece of work is to study the influence of dynamic mechanical properties of MRE on the vibration isolation effect. Tests on dynamic mechanical analysis of MRE structures are performed to obtain experimental results of system stiffness. A fractional rheological model is developed for MRE-based isolation systems, and the model parameters are identified through data fitting of system stiffness in frequency domain. Numerical simulations of this proposed dynamic model are calculated with the predictor-corrector approach, which is verified by comparing theoretical and numerical results of the transmissibility. The influence of model parameters on the isolation effect is analyzed by calculating the transmissibility theoretically and simulating the energy flow numerically. A control strategy is proposed for the application of MRE to protect the foundation or the sensitive equipment against periodic vibrations. The vibration isolation effect is analyzed from the prospect of transmissibility and energy flow. The fuzzy control algorithm is used for the application of MRE to isolate the sensitive equipment against random motions of the ground. The isolation effect is further analyzed by comparing with the passive isolation. Eventually, the feasibility of the fuzzy control algorithm was analyzed considering the response time of MRE material. This paper will contribute to the realization of higher efficiency in MRE-based isolation systems.

2 Model and method

2.1 Modeling of MRE-based isolation system

The vibration isolation system consists of a machine, an MRE-based vibration isolator and a foundation, and the schematic diagram is shown in Fig. 1. The machine placed on the top can be a rotating machine or sensitive equipment, and the foundation located at the bottom can be a fixed foundation or a flexible foundation. The vibration isolator mounted between the machine and the foundation can be an MRE structure in parallel or in series.

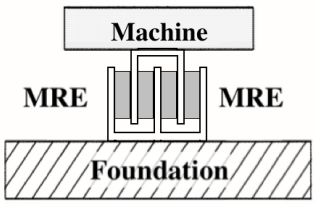

Fig. 1 Schematic diagram of MRE-based isolation system

Because the shear modulus is influenced by the amplitude, frequency and the magnetic field, a constitutive model of MRE is introduced to describe the relation between the force and the displacement in vertical direction, which is the only direction considered in this vibration isolation system. As shown in Fig. 2, the model of MRE-based isolation system is developed from the constitutive model in the paper (Zhu *et al.*, 2021a).

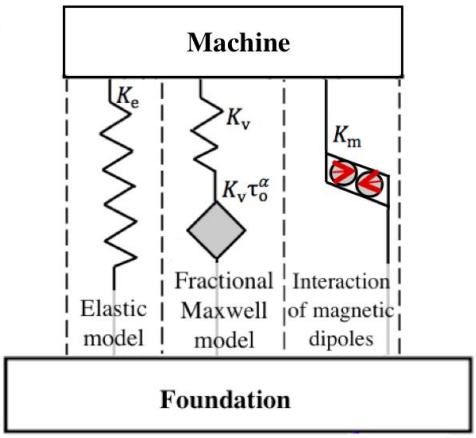

Fig. 2 Schematic configuration for the model of MRE-based isolation system

The total force $F(t)$ for the vibration isolator is comprised of $F_e(t)$, $F_v(t)$ and $F_m(t)$ which represent the elastic, viscoelastic and field-induced forces, respectively. The elastic force $F_e(t)$ is linearly related to the displacement of the MRE-based isolator $\delta(t)$ by

$$F_e(t) = K_e \delta(t) \tag{1}$$

where K_e denotes the stiffness of the elastic model. This parameter can be influenced by the elasticity of the MRE material, and it will contribute to the stiffness of isolation systems.

The viscoelastic force in Fractional Maxwell model $F_v(t)$ can be expressed as

$$F_v(t) = K_v t^a D^a\left[d_n(t)\right] = K_v\left[d(t) - d_v(t)\right] \quad 0 < a < 1 \tag{2}$$

where $\delta_v(t)$ is the displacement of the fractional dashpot in Fractional Maxwell model, D is a differential operator, K_v denotes the stiffness of the Fractional Maxwell model, τ is a relaxation time constant, α is a fractional order. The parameter K_v will contribute to the stiffness of isolation systems, and it can be influenced by the material viscoelasticity, which performs between viscosity and elasticity. The fractional-order differential operator was introduced to describe the viscoelasticity, and the parameter α is influenced by the viscosity of MRE materials. Extreme cases of α=0 and α=1 can represent linear springs and Newton dashpots, respectively. The parameter τ is influenced by the response time of MRE materials, and both the parameters τ and α will contribute to the damping of isolation systems (Poojary and Gangadharan, 2021; Nguyen *et al.*, 2020; Nadzharyan *et al.*, 2018; Zhu *et al.*, 2021a).

As a result of the interaction of magnetic dipoles, the field-induced force $F_m(t)$ can be expressed as

$$F_m(t) = K_m d(t) \tag{3}$$

where K_m denotes the field-induced stiffness which can be controlled by adjusting the magnetic flux density. In an idealized range for control, the magnetic flux density increases linearly with the magnetic field intensity, hence the field-induced stiffness K_m is controllable when the magnetic field is steady and uniform. Outside that range of magnetic field, the increase of magnetic flux density slows down with the further strengthening magnetic field until the saturation magnetization, and the field-induced stiffness K_m cannot be effectively increased anymore (Sapouna *et al.*, 2017; Kaleta *et al.*, 2011). In practice, it is also necessary to consider electromagnetic oscillations because the current changes with time. Considering that the strain affects the magnetic field-induced modulus, the field-induced stiffness K_m is a function of not only the magnetic flux density but also the displacement.

2.2 Parameter identification for MRE structure

The structure consists of aluminum plates and MRE samples 36 × 36 × 8 mm^3, as shown in Fig. 3. The anisotropic MRE samples were comprised of the micron-sized iron particles (carbonyl iron powders sized up to 9 μm, volume concentration of 30%) and the silicone rubber (Wacker Chemie AG, Germany). The mechanical property characterization tests were performed at room temperature (about 22^oC) using Instron Electropuls E1000, which is able to apply and control the harmonic displacement within a wide frequency range. The external magnetic field was produced with cylindrical grade N42 neodymium permanent magnets (E-magnets, UK), and the displacement and the force were recorded in tests. The dynamic mechanical behavior of the MRE structure was recorded by varying frequencies from 1 Hz to 50 Hz, amplitudes from 0.1 mm to 0.5 mm and magnetic fields from 0 to 500 mT, which is in a highly efficient range for vibration control by making full use of energy (Sapouna *et al.*, 2017; Kaleta *et al.*, 2011).

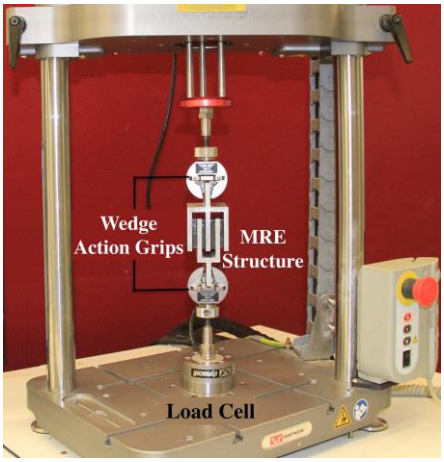

Fig. 3 Experimental setup for parameter identification

The dynamic stiffness of structures, which is complex stiffness, can be measured during tests. Processing experimental data with the software of Wave Matrix, both the real and the imaginary parts of the dynamic stiffness can be obtained. The model parameters K_e, K_v, K_m, τ and α can be identified based on the experimental data of the complex stiffness by optimization. The details of identification procedures and criteria were clarified in this reference (Zhu *et al.*, 2021a). When the excitation amplitude in tests is a maximum of 0.5 mm, and the frequency varies from 1 to 50 Hz, results of parameter identification are listed in Tables 1 and 2. It is found that the stiffness of this MRE structure decreases as the amplitude of excitation increases. As for different excitation amplitudes (from 0.1 mm to 0.5 mm), the parameters τ and α can hardly change, but the parameters K_e, K_v and K_m decrease with increasing amplitudes (at most

10%). Only the influence of magnetic field on the field-induced stiffness K_m is considered, and the influence of magnetic field on other model parameters is relatively small and negligible. When the excitation amplitude is 0.5 mm and the magnetic field varies from 0 to 500 mT, the parameters K_e, K_v, τ and α are the same, the results of identified parameter K_m are listed in Table 2.

Table 1 Results of the parameter identification

K_e (kN/m)	K_v (kN/m)	τ (s)	α
200	180	0.3	0.35

Table 2 Parameter identification for the field-induced stiffness

Magnetic flux density (mT)	0	160	260	400	500
K_m (kN/m)	0	64	104	160	200

Under sinusoidal excitations, the response of MRE material is also a sinusoidal function of the same angular frequency with a certain phase difference. From equation (2), $\delta_v(t)$ can be expressed as

$$d_v(t) = \frac{1}{1+t^a D^a} d(t) \tag{4}$$

The relationship between the force $F(t)$ and the displacement $\delta(t)$ can be obtained with equations (1)-(4).

$$F(t) = K_e d(t) + K_v t^a D^a \left[d_v(t) \right] + K_m d(t) = \left(K_e + \frac{K_v t^a D^a}{1+t^a D^a} + K_m \right) d(t) \tag{5}$$

Applying the Fourier transform, the relationship can be expressed in the frequency domain.

$$F(w) = \left(K_e + \frac{K_v t^a (iw)^a}{1+t^a (iw)^a} + K_m \right) d(w) \tag{6}$$

Substituting $i^\alpha = \cos(\alpha\pi/2) + i\sin(\alpha\pi/2)$ into equation (6), the complex stiffness of this isolation system K^* can be readily found as

$$K^* = K_e + \frac{K_v t^a w^a \left[\cos\left(\frac{ap}{2}\right) + i\sin\left(\frac{ap}{2}\right) \right]}{1+t^a w^a \left[\cos\left(\frac{ap}{2}\right) + i\sin\left(\frac{ap}{2}\right) \right]} + K_m \tag{7}$$

Rationalizing the complex denominator

$$K^* = K_e + \frac{K_v t^a w^a \left[\cos\left(\frac{ap}{2}\right) + i\sin\left(\frac{ap}{2}\right)\right]}{\left[t^a w^a \cos\left(\frac{ap}{2}\right)+1\right] + it^a w^a \sin\frac{ap}{2}} \cdot \frac{\left[t^a w^a \cos\left(\frac{ap}{2}\right)+1\right] - it^a w^a \sin\frac{ap}{2}}{\left[t^a w^a \cos\left(\frac{ap}{2}\right)+1\right] - it^a w^a \sin\frac{ap}{2}} + K_m \quad (8)$$

Separating the real and imaginary parts,

$$K^* = K_e + \frac{K_v t^a w^a \left[\cos\left(\frac{ap}{2}\right) + t^a w^a\right]}{1 + t^{2a} w^{2a} + 2t^a w^a \cos\left(\frac{ap}{2}\right)} + K_m + i\frac{K_v t^a w^a \sin\left(\frac{ap}{2}\right)}{1 + t^{2a} w^{2a} + 2t^a w^a \cos\left(\frac{ap}{2}\right)} \quad (9)$$

Based upon the model parameters in Table 1, the complex stiffness K^* can be fitted by calculating with equation (9). When the excitations and the response are sinusoidal in dynamic mechanical analysis tests, the modulus of the complex stiffness K^* can be measured as the ratio of the force amplitude F_p to the displacement amplitude δ_p. The comparison for the system stiffness is shown in Fig. 4, where the fitted results and the experimental results are in a good agreement. When the standard error ratio $S_e/S_y < 0.35$ and the coefficient of determination $R^2 > 0.90$, the quality of curve fitting can be accepted to be excellent (Zhu *et al.*, 2021a). The details are listed in Table 3. The system stiffness is observed to increase with the frequency. Initially the system stiffness increases linearly with the magnetic field intensity, because the magnetic flux density is proportional to the magnetic field intensity. In this range, the system stiffness can be effectively controlled by adjusting the magnetic field intensity. Above a certain value, the further strengthening magnetic field cannot obviously improve the system stiffness because of the saturation magnetization.

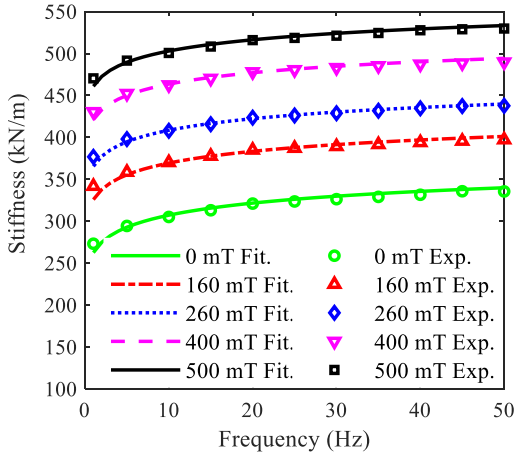

Fig. 4 Fitted results and experimental results of the system stiffness

In case of harmonic excitations, the energy loss per cycle E_v can be calculated by the displacement amplitude δ_p and the imaginary part of system stiffness K^* in equation

(9). The loss energy per cycle can be defined as

$$E_v = p\frac{K_v t^a w^a \sin\left(\frac{ap}{2}\right)}{1+t^{2a}w^{2a}+2t^a w^a \cos\left(\frac{ap}{2}\right)}d_p^p \tag{10}$$

Table 3 The goodness-of-fit

Magnetic field (mT)	0	160	260	400	500
Standard error ratio	0.9980	0.9993	0.9991	0.9988	0.9975
Coefficient of determination	0.0583	0.0331	0.0400	0.0458	0.0435

The fractional order α is mainly controlled by the components in the manufacture, and the fractional order α reflects the viscoelasticity in this vibration isolation system. The influence of fractional order α on the system stiffness can be observed in Fig. 5 (a). The system stiffness can be reduced as the fractional order α increases at frequencies below 10 Hz, and as the fractional order α decreases at frequencies above 10 Hz. The system stiffness commonly influences the resonance frequency, so the results of system stiffness in Fig. 5 (a) can be used for the following analysis of resonance frequency. The influence of fractional order α on the loss energy is shown in Fig. 5 (b), where the loss energy per cycle E_v can be increased by increasing the fractional order α at frequencies below 30 Hz. It indicates that the ability of MRE to dissipate the energy of deformation increases as the fractional order α increases at frequencies below 30 Hz. The loss energy affects the viscoelasticity in this MRE structure, the results of loss energy in Fig. 5 (b) can be also observed in the following power flow analysis.

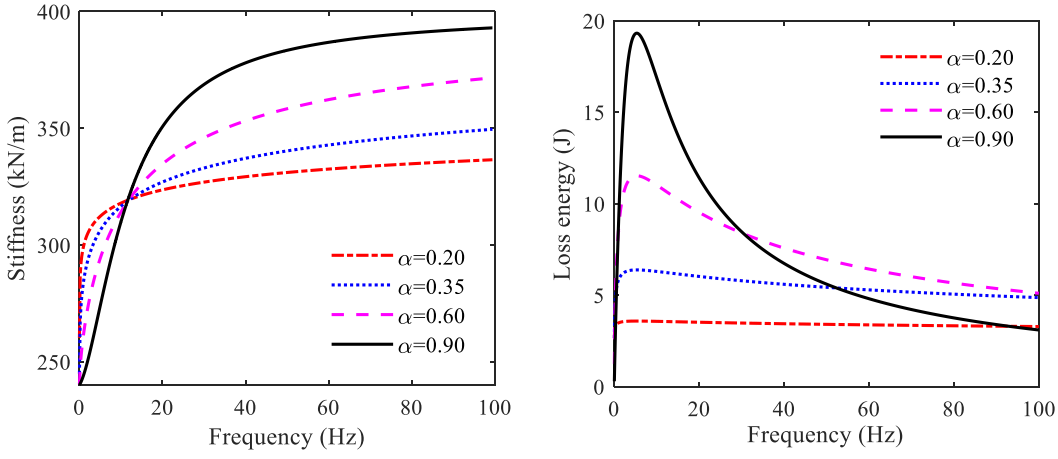

(a) (b)

Fig. 5 Influence of the fractional order on (a) the system stiffness and (b) the loss energy

3 Vibration control against harmonic force

3.1 Basics for transmissibility and energy flow

When the excitation is harmonic force $F_0(t) = F_0 \sin \omega t$ exerted on the machine in Fig. 2, the differential equations of motion in this vibration isolation system can be expressed as

$$\begin{aligned} &m\ddot{x}(t) + K_e x(t) + K_v \tau^\alpha D^\alpha x_v(t) + K_m x(t) = F_0 \sin \omega t \\ &x_v(t) + \tau^\alpha D^\alpha x_v(t) = x(t) \end{aligned} \tag{11}$$

where $\omega = 2\pi f$, ω and f are the angular frequency and the frequency, respectively; m and $x(t)$ are the mass and the displacement of the machine, respectively; $x_v(t)$ is the displacement of the fractional dashpot. Because the infinite foundation is fixed, the relationship between the displacements $x(t) = \delta(t)$ and $x_v(t) = \delta_v(t)$ can be found.

The transmissibility, the ratio of forces or displacements, is commonly investigated for vibration isolation systems. In case of that the excitation is harmonic force in this vibration isolation system, the transmissibility is defined as a ratio of forces. Exactly speaking, it is a ratio of the response amplitude F_p to the excitation amplitude F_0.

$$I = \frac{F_p}{F_0} \tag{12}$$

Substituting the complex stiffness K^* into the equation (11), the transmissibility of this isolation system λ can be expressed as

$$I = \frac{\left|K^*\right|}{\left|K^* - m\omega^2\right|} \tag{13}$$

Introducing the real and imaginary components in equation (9) to calculate magnitudes in equation (13), the transmissibility λ can be further expressed.

$$I = \frac{\sqrt{\left(K_e + \dfrac{K_v t^\alpha \omega^\alpha \left(\cos\left(\dfrac{\alpha\pi}{2}\right) + t^\alpha \omega^\alpha\right)}{1 + t^{2\alpha}\omega^{2\alpha} + 2t^\alpha \omega^\alpha \cos\left(\dfrac{\alpha\pi}{2}\right)} + K_m\right)^2 + \left(\dfrac{K_v t^\alpha \omega^\alpha \sin\left(\dfrac{\alpha\pi}{2}\right)}{1 + t^{2\alpha}\omega^{2\alpha} + 2t^\alpha \omega^\alpha \cos\left(\dfrac{\alpha\pi}{2}\right)}\right)^2}}{\sqrt{\left(K_e + \dfrac{K_v t^\alpha \omega^\alpha \left(\cos\left(\dfrac{\alpha\pi}{2}\right) + t^\alpha \omega^\alpha\right)}{1 + t^{2\alpha}\omega^{2\alpha} + 2t^\alpha \omega^\alpha \cos\left(\dfrac{\alpha\pi}{2}\right)} + K_m - m\omega^2\right)^2 + \left(\dfrac{K_v t^\alpha \omega^\alpha \sin\left(\dfrac{\alpha\pi}{2}\right)}{1 + t^{2\alpha}\omega^{2\alpha} + 2t^\alpha \omega^\alpha \cos\left(\dfrac{\alpha\pi}{2}\right)}\right)^2}} \tag{14}$$

Considering couplings and interactions in dynamic systems, the power flow analysis combines the effects of both the force and the velocity to describe the dynamic behavior. The principle for energy flow approach is based on the universal law of

energy conversation and transformation, and the limitations on separately analyzing forces and responses can be overcome with this method (Xing, 2015). As a time averaged product of velocity and force, the energy flow <*P*> transmitted in this MRE-based isolation system can be defined as the power of the force *F*(*t*) transmitted to the foundation.

$$< P >= \frac{1}{T}\int_{t_0}^{t_0+T} \dot{x}(t)F(t)\,dt \tag{15}$$

where T is a time period and t_0 is an initial time.

3.2 Parameter analysis and method verification

Considering the results of parameter identification for the MRE structure, the vibration isolation system can be designed with MRE structures in parallel herein for high system stiffness and in series for low system stiffness, such as laminated structures of MRE and steel layers (Zhu *et al.*, 2021b; Eem *et al.*, 2019; Li *et al.*, 2019). The system parameters are set to m = 20 kg, F_0 = 20 N, K_e = 200 kN/m, K_v = 180 kN/m and τ = 0.3 s, respectively. According to equation (14), the transmissibility of this isolation system λ can be calculated theoretically for parameter analysis.

The influence of the field-induced stiffness K_m on the transmissibility in frequency domain is shown in Fig. 6 (a). As the field-induced stiffness K_m increases from 0 to 200 kN/m, the resonance frequency increases from 23.5 to 30.5 Hz, so the resonance frequency is shifted by 29.8%; the maximum peek transmissibility at resonance frequencies increases from 12.6 to 17.1 (1.10 dB to 1.23 dB). It can be accepted that effective isolation requires the transmissibility less than unity, and the effectiveness of vibration isolation can be improved by reducing the maximum peek transmissibility or the natural frequency. From this perspective of view, the low field-induced stiffness K_m is beneficial to the effectiveness of isolation.

The influence of the fractional order α on the transmissibility in frequency domain is shown in Fig. 6 (b). In this MRE-based isolation system, when the fractional order α increases from 0.2 to 1.0, the resonance frequency increases from 22.25 to 24.75 Hz, which results from the increasing system stiffness at frequencies above 10 Hz as shown in Fig. 5, and the maximum peek transmissibility decreases from 20.4 to 6.8 (1.31 dB to 0.83 dB). The low resonance frequency and transmissibility are beneficial to the effectiveness of vibration isolation. In accordance with results shown in Fig. 5, at frequencies below 30 Hz the ability to dissipate energy increases as the fractional order α increases, so the maximum peek values of transmissibility can be reduced by

increasing the fractional order α.

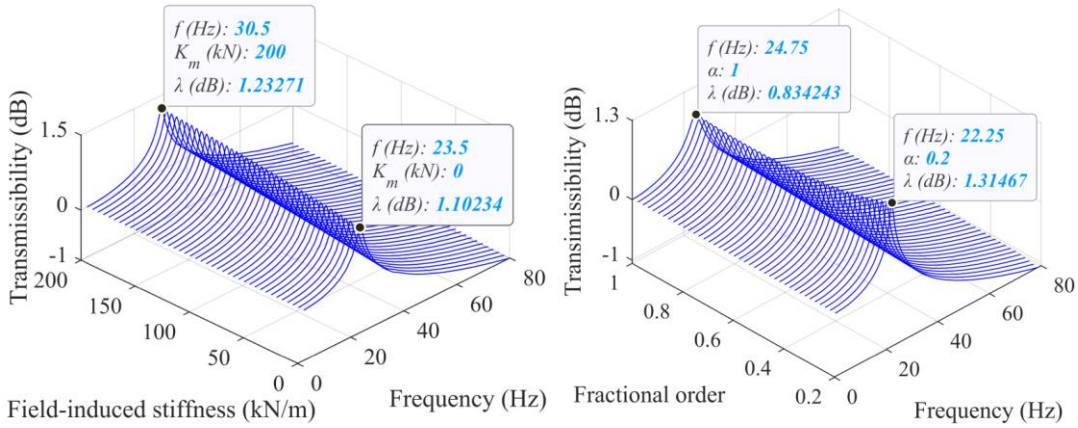

(a) (b)

Fig. 6 Influence of (a) the field-induced stiffness and (b) the fractional order on the transmissibility in frequency domain

Because there is no theoretical result of the energy flow <*P*> in this MRE-based isolation system, a numerical study is necessary to investigate the energy flow <*P*>. In order to examine the method of numerical simulation, the numerical result of transmissibility is calculated to compare with the theoretical result. The Caputo derivative is chosen for the simulation, because the initial conditions for Caputo derivative cases commonly have well understood physical meanings and can be measured in practice (Diethelm *et al.*, 2002). By using the predictor-corrector approach, the numerical solution of Caputo fractional differential equation (11) is carried out to analyze the transmissibility of this isolation system λ as defined in equation (12). The details of calculation method are illustrated in the reference (Zhu *et al.*, 2021a). As shown in Figs. 7 and 8, the numerical results of the transmissibility are compared with the theoretical results obtained in Figs. 6 (a) and (b). The predictor-corrector approach is verified with the good agreement between the theoretical results and the numerical results in frequency domain. Then this reliable method of numerical simulation can be employed in time domain to observe the performance of this MRE-based isolation system when the experiment is absent.

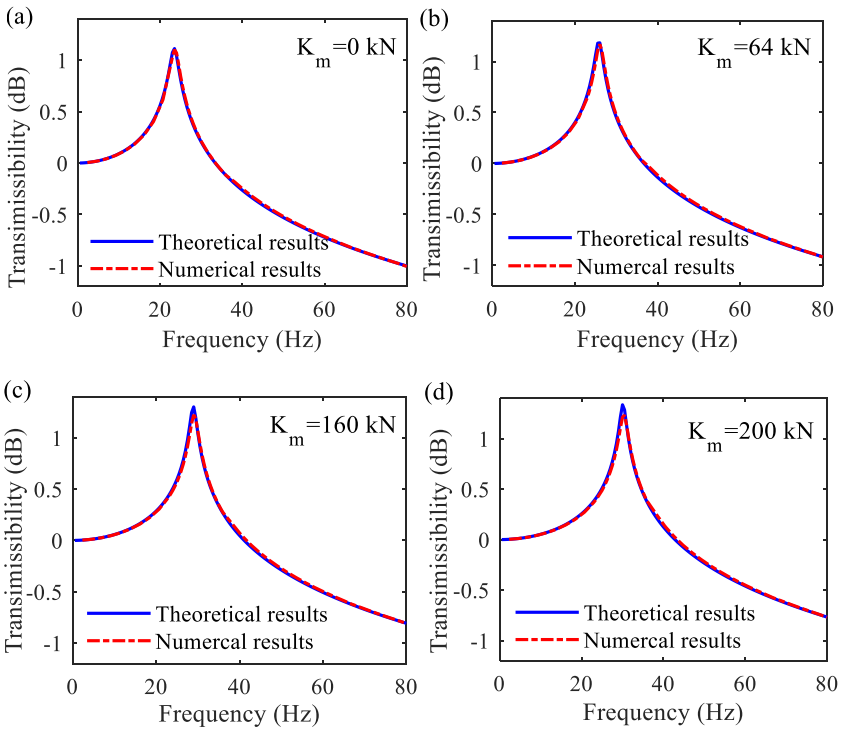

Fig. 7 Theoretical results and numerical results of the transmissibility with various field-induced stiffness: (a) 0 kN, (b) 64 kN, (c) 160 kN and (d) 200 kN

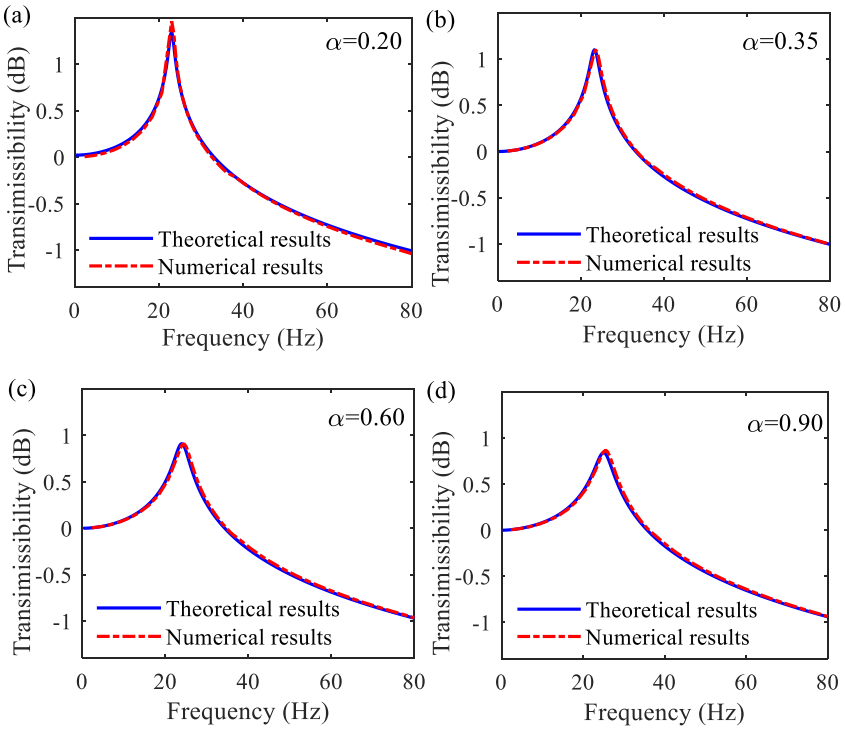

Fig. 8 Theoretical results and numerical results of the transmissibility with various fractional orders: (a) 0.2, (b) 0.35, (c) 0.6 and (d) 0.9

The numerical solution of equation (11) is carried out to analyze the energy flow <*P*> as defined in equation (15). The influence of the field-induced stiffness K_m and the

fractional order α on the energy flow in frequency domain are shown in Figs. 9 (a) and (b), respectively. When the field-induced stiffness K_m increases from 0 to 200 kN/m, the maximum value of energy flow, which is about 18 W, changes very slightly. As the fractional order α increases from 0.2 to 1.0, the maximum value of energy flow decreases from 34.7 to 10.9 W. The maximum peek values of energy flow can be reduced by increasing the fractional order α, which is in accordance with results shown in Fig. 5. At frequencies below 30 Hz, as the fractional order α increases, the ability to dissipate energy in this MRE structure also increases.

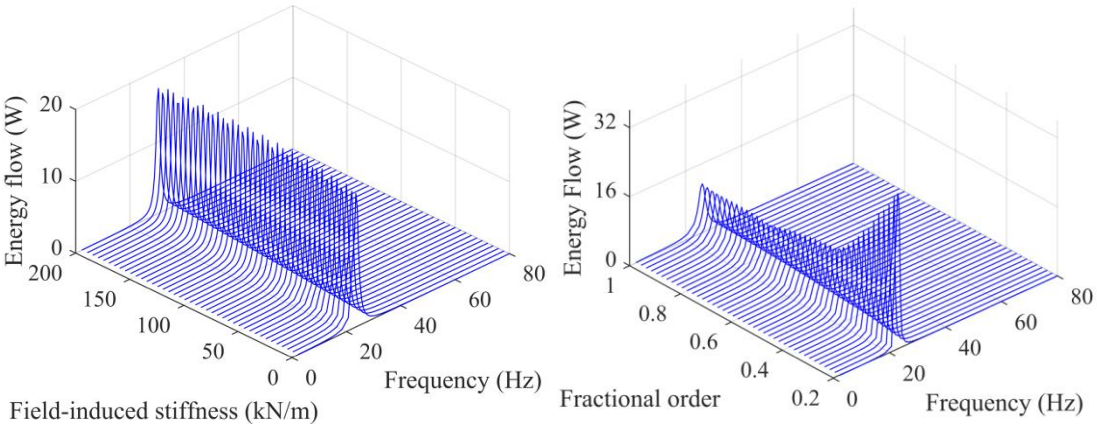

(a) (b)

Fig. 9 Influence of (a) the field-induced stiffness and (b) the fractional order on the energy flow in frequency domain

3.3 Vibration control strategy and isolation effect

It is found that when the magnetic flux density is above 500 mT, the system stiffness cannot be effectively improved with the further strengthening magnetic field because of the saturation magnetization (Sapouna *et al.*, 2017; Kaleta *et al.*, 2011). Considering the influence of the field-induced stiffness in Fig. 7 (a), the two curves of transmissibility in magnetic field of 0 and 500 mT intersect at one point. It means at that frequency the transmissibility in magnetic field of 0 and 500 mT is the same, and this frequency is named as a coincidence frequency f_{co}. In this MRE-based isolation system, the energy flow at a coincidence frequency is almost the same in magnetic field of 0 and 500 mT as well. The reduced transmissibility and energy flow can be achieved through a frequency dependent magnetic field, and the control strategy based on the coincidence frequency f_{co} can be expressed as

$$B(f)=\begin{cases} 0 & (f > f_{co}) \\ 500\ \text{mT} & (f < f_{co}) \end{cases} \tag{16}$$

where B is the magnetic flux density of the controllable magnetic field.

The calculation of isolation effect is carried out in controllable magnetic fields, as shown in Figs. 10 (a) and (b). The maximum values of transmissibility and energy flow can be observed to occur at coincidence frequencies. When the coincidence frequency increases from 26 to 29 Hz, the maximum peek transmissibility increase from 3.7 to 4.0 (0.57 dB to 0.60 dB), and the maximum value of energy flow into the foundation increases from 0.8 to 4.0 W. Comparing with the system in a zero magnetic field, the transmissibility is reduced by 48.1 ~ 87.2%, and the energy flow into the foundation is reduced by 63.3 ~ 97.7%.

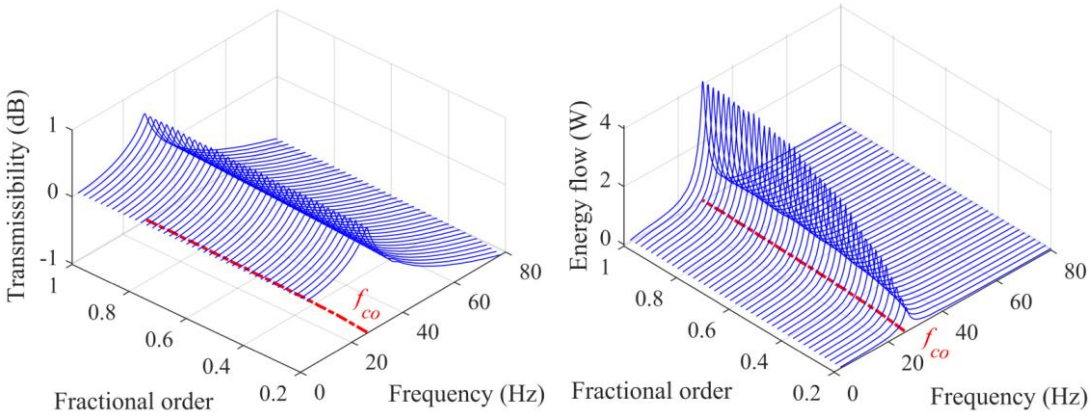

Fig. 10 Isolation effect against harmonic force on (a) the transmissibility and (b) the energy flow in frequency domain

4 Vibration control against foundation motion

4.1 Isolation effect against harmonic motion

When the excitation in Fig. 2 is harmonic motion of the foundation $x_0(t) = X_0 \sin \omega t$, such as the waves, the differential equations of motion in this vibration isolation system can be expressed as

$$\begin{aligned} &m\ddot{x}(t) + K_e\delta(t) + K_v\tau^\alpha D^\alpha\delta_v(t) + K_m\delta(t) = 0 \\ &\delta(t) = \delta_v(t) + \tau^\alpha D^\alpha\delta_v(t) \end{aligned} \tag{17}$$

When the displacement of the foundation is $x_0(t)$ and the relative displacement of the MRE-based isolator is $\delta(t)$, the displacement of the machine can be also expressed as $x(t) = \delta(t) + x_0(t)$.

In case of that the excitation is a harmonic motion of the foundation, the response motion of the machine is also a sinusoidal function of the same angular frequency. The transmissibility, which is the non-dimensional ratio of the response amplitude to the

excitation amplitude, can be defined as a ratio of displacements herein. When the displacement amplitude of the machine is denoted as X_p to study the vibration isolation system, the transmissibility is the ratio of the response amplitude X_p to the excitation amplitude X_0.

$$T = \frac{X_p}{X_0} \tag{18}$$

The energy flow <P> can be defined as the power of the force $F(t)$ transmitted to the machine and be expressed as the same as equation (15).

The system parameters are set to m = 20 kg, X_0 = 0.5 cm, K_e = 200 kN/m, K_v = 180 kN/m and τ =0.3 s. The numerical solution of Caputo fractional differential equation (17) is carried out with the predictor-corrector approach to analyze this MRE-based isolation system. The reduced transmissibility and energy flow is achieved with the same control strategy as illustrated in equation (16), and the simulation of isolation effect is carried out in controllable magnetic fields. Figs. 11 (a) and (b) show the numerical results, as the coincidence frequency increases from 26.5 to 28.5 Hz, the maximum peek transmissibility increase from 3.8 to 4.4 (0.58 dB to 0.64 dB), and the maximum value of energy flow into the machine increases from 1.6 to 2.5 W. Comparing with the system in a zero magnetic field, the transmissibility is reduced by 69.1 ~ 74.9%, and the energy flow into the machine is reduced by 87.0 ~ 92.1%.

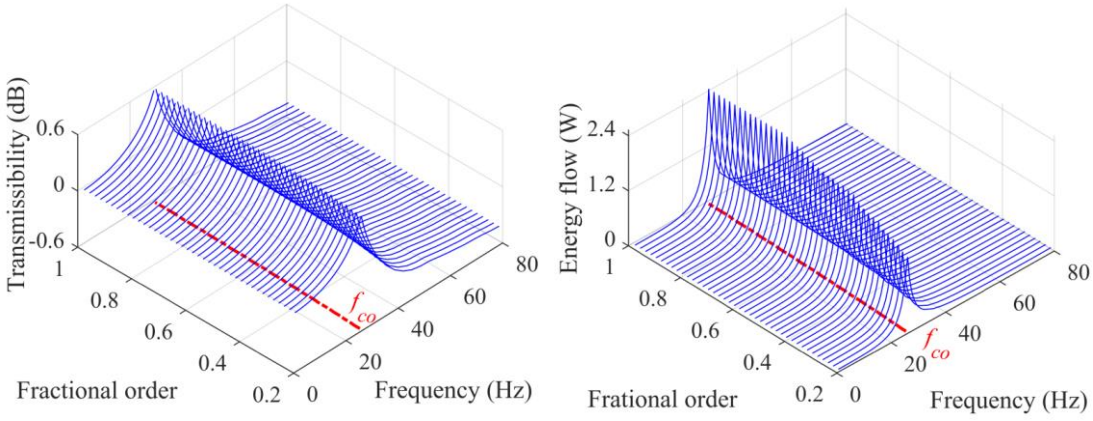

Fig. 11 Isolation effect against foundation motion on (a) the transmissibility and (b) the energy flow in frequency domain

4.2 Isolation effect against random motion

The differential equation (17) is not limited to harmonic excitations. When the nonlinearities that result from the amplitude dependent stiffness and the mechano-magnetic coupling effect are not considered, the predictor-corrector approach can be

also employed to numerically solve differential equations under random excitations. A common method to address the uncertainty and the nonlinear phenomenon of systems is the fuzzy logical control algorithm. The simple output signals and calculation can effectively reduce the time delay of control algorithms to the utmost extent (Fu *et al.*, 2018; Nguyen *et al.*, 2018a). The displacement $x(t)$ and the velocity $\dot{x}(t)$ of the MRE-based isolator are selected to serve as input signals, and the motion of the machine is calculated for the transmissibility. The details for the control algorithm are described in equation (19). The stiffness is physically increased as the machine leaves from the equilibrium position and decreased as the machine moves towards the equilibrium position.

$$B\left(x,\dot{x}\right)=\begin{cases} 0 & \left(x\times\dot{x}<0\right) \\ 500\ \text{mT} & \left(x\times\dot{x}>0\right) \end{cases} \tag{19}$$

Considering the common vibrations range from 3 to 20 Hz in the marine environment, the band-limited Gaussian noise and the multi-frequency vibration are employed as the motion excitation of the foundation to verify the effectiveness of the MRE-based isolation system. The time delay due to controllers and current drivers is not considered for simplification, and the delay control can be utilized to compensate the time delay.

The responses of the machine in zero and controllable magnetic fields are compared with the motion of the foundation to illustrate the isolation efficiency, as shown in Figs. 12 and 13. The peak and the root mean square (RMS) values of the displacement of the machine under band-limited Gaussian noise (3~20 Hz) and multi-frequency vibration (3 Hz, 8 Hz and 20 Hz) are calculated in Fig. 14. Compared with the passive control in a zero magnetic field, the peak and the RMS values for the band-limited Gaussian noise are reduced by 30.14% and 26.95%, respectively; the peak and the RMS values for the multi-frequency vibration are reduced by 22.39% and 27.50%, respectively. The vibration isolation performance can be enhanced by the MRE isolator with fuzzy logical control, and it can be deduced that the larger MR effect can further demonstrate the enhancement.

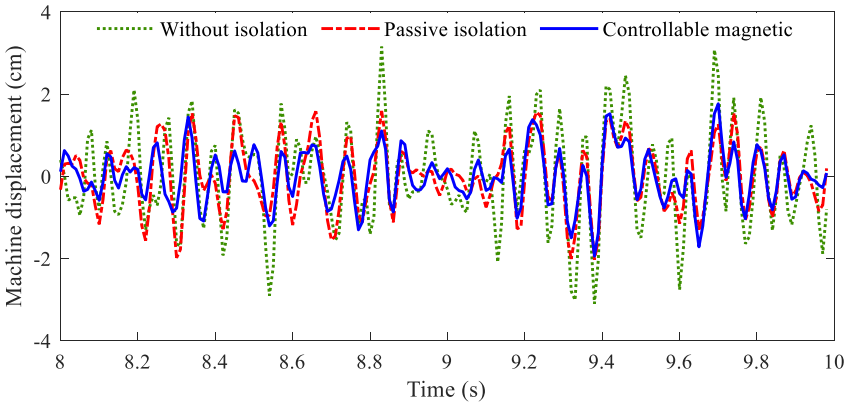

Fig. 12 Displacement of the machine with no isolation, passive isolation and fuzzy logical controllable magnetic filed for the Band-limited Gaussian noise

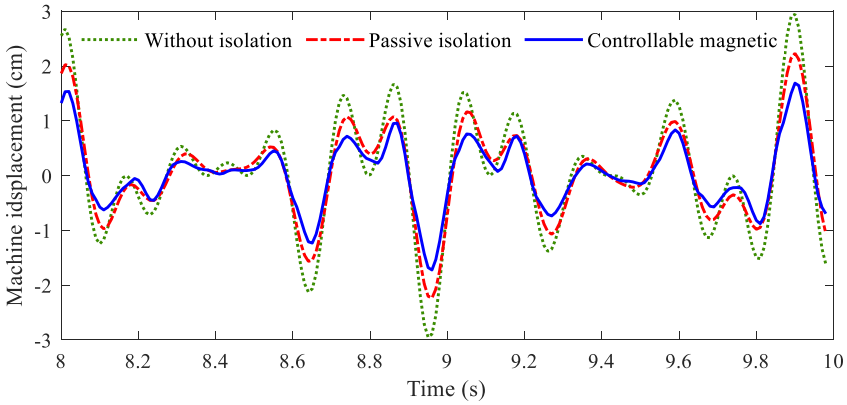

Fig. 13 Displacement of the machine with no isolation, passive isolation and fuzzy logical controllable magnetic filed for the Multi-frequency vibration

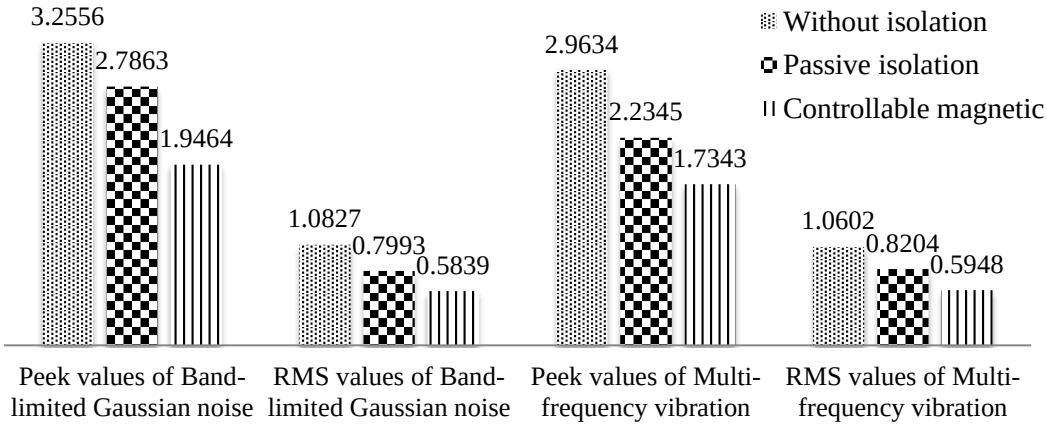

Fig. 14 Peak and RMS values of the displacement of the machine (cm)

For the fuzzy control strategy, the controllable magnetic field can effectively respond to the excitation only if the frequency of control instructions is mathematically four times larger than the frequency of excitations (Wang and Kari, 2019b).

Considering the response time of MRE materials is at least 12.5 ms (Zhu *et al.*, 2018), the frequency of control instructions is at most 80 Hz. Therefore, the efficiency of the MRE-based isolation system can be effectively improved by the fuzzy logical control when both the highest frequency component of excitations and the resonance frequency of systems are lower than 20 Hz.

5 Conclusions

In this study, a fractional rheological model was developed to investigate the isolation effect of MRE-based isolation systems. The dynamic mechanical analysis tests for MRE structures were performed to validate this proposed dynamic model, and the model parameters were identified by fitting the experimental data on system stiffness in frequency domain. The method of numerical simulation was verified by calculating the transmissibility both theoretically and numerically, and the numerical results displayed an excellent agreement with the theoretical results. Considering material elasticity and viscosity, the influence of model parameters on isolation effect was analyzed by calculating the transmissibility and the energy flow. A control strategy based on the coincidence frequency was developed for this MRE-based isolation system to protect the foundation or the sensitive equipment against periodic vibrations. Comparing with the passive isolation system, the force transmissibility and the energy flow transmitted to the foundation can be reduced with the controllable magnetic field by 48% and 81% at least, respectively; the displacement transmissibility and the energy flow transmitted to the sensitive equipment can be reduced by more than 69% and 87%, respectively.

The fuzzy control algorithm was employed to isolate the sensitive equipment against random motions. Comparing with the passive isolation system, the peak and the RMS values of the displacement can be reduced by at least 22% and 27%, respectively. Considering the response time of MRE, the fuzzy control algorithm can only exhibit an enhanced isolation effect in low frequency region. The dynamic analysis and the control strategy can be verified by further experimental research to facilitate higher efficiency of MRE-based isolation systems.

Acknowledgement

This study was funded by National Natural Science Foundation of China (grant numbers 12002267, 12172279, 11972282 and 12172247) and Science Foundation of Education Department of Shaanxi (grant number 20JK0777).

References

Bai XX, Cai FL and Chen P (2019) Resistor-capacitor (RC) operator-based hysteresis model for magnetorheological (MR) dampers. *Mechanical Systems and Signal Processing* 117: 157–169.

Behrooz M, Wang X and Gordaninejad F (2014) Performance of a new magnetorheological elastomer isolation system. *Smart Materials and Structures* 23(4): 045014.

Bian Y, Liang X and Gao Z (2018) Vibration reduction for a flexible arm using magnetorheological elastomer vibration absorber. *Shock Vibration* 2018: 9723538.

Chen L, Gong XL and Li WH (2007) Microstructures and viscoelastic properties of anisotropic magnetorheological elastomers. *Smart Materials and Structures* 16(6): 2645-2649.

Davis LC (1999) Model of Magnetorheological Elastomers. *Journal of Applied Physics* 85(6): 3348-3351.

Diethelm K, Ford NJ and Freed AD (2002) A Predictor-Corrector Approach for the Numerical Solution of Fractional Differential Equations. *Nonlinear Dynamics* 29(4): 3-22.

Eem SH, Koo JH and Jung HJ (2019) Feasibility study of an adaptive mount system based on magnetorheological elastomer using real-time hybrid simulation. *Journal Intelligent Material Systems and Structures* 30(5): 701-707.

Fu J, Dai Z, Yang Z, Lai JJ and Yu M (2020) Time delay analysis and constant time-delay compensation control for MRE vibration control system with Fuzzy controller and multiple-frequency excitation. *Smart Materials and Structures* 29(1): 014001.

Fu J, Li P, Liao G, Lai JJ and Yu M (2018) Active/semi-active hybrid isolation system with fuzzy switching controller. *Journal Intelligent Material Systems and Structures* 29(1): 101-115.

Graczykowski C and PawlOwski P (2017) Exact physical model of magnetorheological damper. *Applied Mathematical Modelling* 47: 400-424.

Ibrahim RA (2008) Recent advances in nonlinear passive vibration isolators. *Journal of Sound and Vibration* 314(3-5): 371-452.

Jolly MR, Carlson JD and Munoz BC (1996) A model of the behavior of magnetorheological materials. *Smart Materials and Structures* 5(5): 607–614.

Kaleta J, Królewicz M and Lewandowski D (2011) Magnetomechanical properties of anisotropic and isotropic magnetorheological composites with thermoplastic elastomer matrices. *Smart Materials and Structures* 20(8): 085006.

Kumbhar SB, Chavan SP and Gawade SS (2018) Adaptive tuned vibration absorber based on magnetorheological elastomer-shape memory alloy composite. *Mechanical Systems and Signal Processing* 100: 208-223.

Li Y and Li J (2019) Overview of the development of smart base isolation system featuring magnetorheological elastomer. *Smart Materials and Structures* 24(1): 37-52.

Liu C, Jing X, Daley S and Li F (2015) Recent advances in micro-vibration isolation. *Mechanical Systems and Signal Processing* 56-57: 55-80.

Nadzharyan TA, Kostrov SA, Stepanov GV and Kramarenko EY (2018) Fractional rheological models of dynamic mechanical behavior of magnetoactive elastomers in magnetic fields. *Polymer* 142(4): 316-329.

Nguyen SD, Lam BD, Nguyen QH and Choi SB (2018a) A fuzzy-based dynamic inversion controller with application to vibration control of vehicle suspension system subjected to uncertainties. *Journal of Systems and Control Engineering* 232(9): 1103-1119.

Nguyen XB, Komatsuzaki T, Iwata Y and Asanuma H (2018b) Robust adaptive controller for semi-active control of uncertain structures using a magnetorheological elastomer-based isolator. *Journal of Sound and Vibration* 434: 192–212.

Nguyen XB, Komatsuzaki T and Zhang N (2020) A nonlinear magnetorheological elastomer model based on fractional viscoelasticity, magnetic dipole interactions, and adaptive smooth Coulomb friction. *Mechanical Systems and Signal Processing* 141: 106438.

Poojary UR and Gangadharan KV (2022) Fractional-order viscoelastic modeling of the magnetic field dependent transmissibility response of MRE isolator. J*ournal of Intelligent Material Systems and Structures* DOI:10.1177/1045389X221087172.

Poojary UR and Gangadharan KV (2021) Material modeling of frequency, magnetic field and strain dependent response of magnetorheological elastomer. *Journal of Materials Science* 56(28): 15752–15766.

Qian LJ, Xin FL, Bai XX and Wereley NM (2017) State observation based control algorithm for dynamic vibration absorbing systems featuring magnetorheological elastomers: principle and analysis. *Journal of Intelligent Material Systems and Structures* 28(18): 2539–2556.

Sapouna K, Xiong YP and Shenoi RA (2017) Dynamic mechanical properties of isotropic / anisotropic silicon magnetorheological elastomer composites. *Smart Materials and Structures* 26(10): 115010.

Wan YX, Xiong YP and Zhang SM (2019) Temperature effect on viscoelastic properties of anisotropic magnetorheological elastomers under compression. *Smart Materials and Structures* 28(1): 015005.

Wang B and Kari L (2019a) A nonlinear constitutive model by spring, fractional derivative and modified bounding surface model to represent the amplitude, frequency and the magnetic dependency for Magneto-sensitive rubber. *Journal of Sound and Vibration* 438: 344-352.

Wang B and Kari L (2019b) Modeling and vibration control of a smart vibration isolation system based on magneto-sensitive rubber. *Smart Materials and Structures* 28(6): 065026.

Wu M, He Y and She JH (2010) Stability Analysis and Robust Control of Time-Delay System, Berlin: Springer.

Xin FL, Bai XX and Qian LJ (2017) Principle, modeling and control of a magnetorheological elastomer dynamic vibration absorber for powertrain mount systems of automobiles. *Journal of Intelligent Material Systems and Structures* 28(16): 2239–2254

Xing JT (2015) Energy Flow Theory of Nonlinear Dynamical Systems with Applications, Berlin: Springer.

Yan LX, Xuan SH and Gong XL (2018) Shock isolation performance of a geometric anti-spring isolator. *Journal of Sound and Vibration* 413: 120-143.

Yang J, Du H and Li W (2013) Experimental study and modeling of a novel magnetorheological elastomer isolator. *Smart Materials and Structures* 22(11): 117001.

Yang J, Sun SS, Du H, Li WH, Alici G and Deng HX (2014) A novel magnetorheological elastomer isolator with negative changing stiffness for vibration reduction. *Smart Materials and Structures* 23(10): 105023.

Yu Y, Li YC and Li JC (2015) Parameter identification of a novel strain stiffening model for magnetorheological elastomer base isolator utilizing enhanced particle swarm optimization. *Journal of Intelligent Material Systems and Structures* 26(18): 2446–2462.

Yu T, Rui X, Yang F and Hao B (2019) Development of a MRE isolation system for strapdown inertial measurement unit. *Mechanical Systems and Signal Processing* 117: 553-568.

Yuan L, Sun S, Pan Z, Ding D, Gienke O and Li WH (2019) Mode coupling chatter suppression for robotic machining using semi-active magnetorheological elastomers absorber, *Mechanical Systems and Signal Processing* 117: 221-237.

Zhu G, Li Z, Xiong Y, Xiao L and Li M (2019) Dynamic Mechanical Properties of Magnetorheological Elastomers: Experiment and Modelling. *IOP Conference Series: Materials Science and Engineering* 559(1): 012001.

Zhu G, Xiong Y, Li Z, Xiao L, Li M and Bai X (2021a) A nonlinear dynamic model of magnetorheological elastomers in magnetic fields based on fractional viscoelasticity. *Journal of Intelligent Material Systems and Structures* 32(2): 228-239.

Zhu M, Fu J and Li W (2021b) Design and co-optimization of a laminated isolation bearing based on magnetorheological elastomer. *Mechanical Systems and Signal Processing* 159: 107843.

Zhu M, Yu M, Qi S and Fu J (2018) Investigations on response time of magnetorheological elastomer under compression mode. *Smart Materials and Structures* 27(5): 055017.